Basic Performance Tests of the MILL Intravascular CO_2 Removal Catheter*

Christoph Janeczek, Benjamin Lukitsch, Florentine Huber-Dangl, Alen Karabegovic, Christian Jordan, Bahram Haddadi, Roman Ullrich, Claus Krenn, Margit Gfoehler, Michael Harasek

— Currently available treatment methods for acute lung failure show high rates of complications. There is an urgent need for alternative treatment methods. A catheter device which can be minimal invasively inserted into the vena cava for intracorporeal gas exchange was developed. Main components of the device are a drive unit and a membrane module. In this study, the flow behavior in a vena cava model with inserted catheter prototype was investigated in experiments and basic computational fluid dynamic (CFD) simulations. Main findings are that the miniature blood pump has suitable characteristics and generates sufficient power to overcome the pressure drop induced in the membrane module, and that the design of the membrane outlet might be critical to avoid additional pressure losses. Parts manufactured with a high resolution 3D printer have proven to be suitable for the prototyping process.

I. INTRODUCTION

Lung diseases are among the most relevant topics in medical treatment of patients [1] and lead to high mortality rates [2]. Patients with severe forms of respiratory failure frequently require mechanical ventilation to support their lung function [3]. Although life-saving, this technique often results in application of high tidal volumes and high alveolar pressures to maintain an adequate gas exchange. The associated mechanical stress and strain on the lungs leads to an aggravation of alveolar damage and development of acute respiratory distress syndrome [4], which bears a mortality rate of more than 40 % [5]. Additional problematic situations can arise during weaning after the treatment [6].

Alternatively, full lung support membrane oxygenation can be applied. Standard membrane oxygenators need a surface area of about two square meters to achieve sufficient gas exchange for an adult patient. Consequently, due to the required size, full lung support can only be supplied extracorporeally, meaning that high blood quantities must be guided in and out of the body which can lead to a number of complications including bleeding, thrombus formation, emboli and infection [7].

*Research supported by the Austrian Research Promotion Agency (FFG). Project: MILL – Minimal Invasive Liquid Lung. Project number: 857859.

C. Janeczek, is with the Institute of Engineering Design and Logistics Engineering, TU Wien, Vienna, AUT (phone: +43 (1) 58801 - 307 45; fax: +43 (1) 58801 – 930745; e-mail: christoph.janeczek@tuwien.ac.at).

B. Lukitsch, M. Gfoehler, F. Huber-Dangl, C. Jordan, B. S: Haddadi, A. Karabegovic, M. Harasek are with the TU Wien, Vienna, AUT (e-mail: benjamin.lukitsch@tuwien.ac.at, margit.gfoehler@tuwien.ac.at, florentine.huber-dangl@tuwien.ac.at, christian.jordan@tuwien.ac.at, bahram.haddadi@tuwien.ac.at, alen.karabegovic@tuwien.ac.at, michael.harasek@tuwien.ac.at).

C. Janeczek, B. Lukitsch, F. Huber-Dangl, A. Karabegovic R. Ullrich, C. Krenn are with CCore Technology GmbH, Vienna, AUT (e-mail: roman.ullrich@ccore.at, claus.krenn@ccore.at).

Membrane oxygenators use hollow fibers for gas exchange. Blood flows on the shell side of the fibers while the lumen is swept, most commonly with O_2. Due to the partial pressure difference, CO_2 is transported from the blood through the membrane into the sweep gas. O_2 perfuses in the other direction, out of the hollow fiber membrane and into the blood.

An alternative to currently available treatment methods is the use of a minimal invasive intracorporeal system for gas exchange. It is designed as a catheter that can be inserted directly into the vena cava and consequently, no blood needs to be guided outside the patient's body, omitting the mentioned complications. However, due to physiological size restrictions for the catheter, only partial removal of carbon dioxide can be achieved with current intracorporeal systems [8]–[10].

Aim of the project MILL – "Minimal Invasive Liquid Lung" is to develop an intravascular membrane catheter for gas exchange in venous blood with an integrated propulsion system. The goal is to remove at least 20 % of metabolic CO_2 production, which equals to about 40 ml/min. As a novelty, liquid perfluorocarbon (PFC) is used to sweep the fiber lumens. Using liquid PFC avoids the risk of gas embolism in case of leakage. PFCs have high CO_2 solubility of up to 207% (v/v at 25 °C) [11] and are used as blood substitutes in clinical applications [12].

A miniaturized blood pump is integrated at the inlet of the membrane module to compensate for the pressure loss induced by the catheter in the vena cava and the hollow fiber packing. The pump is necessary to ensure adequate blood flow of about 0.7 to 1.2 L/min for sufficient gas exchange.

The aim of this study is to verify whether the designed blood pump can provide required blood flows while investigating the blood flow behavior in a vena cava model with inserted catheter prototype using in-vitro experiments in a test loop (Fig. 1) and basic CFD simulations. Additionally, it is investigated whether rapid prototyping with a DLP resin printer is suitable for manufacturing main parts of the intravascular membrane catheter.

II. MATERIALS AND METHODS

A. Gas exchange catheter

Basic set-up of the gas exchange catheter is shown in Fig. 2. A multi lumen tube enters the catheter and provides the device with wires for power and control as well as PFC supply hoses. The drive unit is positioned in the up-stream end of the catheter housing (Fig. 1). Here the torque is transmitted from the motor (Maxon ECX8) to the blood

pump via a patented magnetic coupling [13]. This allows hermetic separation of blood guiding parts and elements that are not in contact with blood.

Between the motor and the blood pump three suction inlets (Fig.1, 1) are trimmed in the catheter shell. Blood is pumped through these peripheral inlets into the membrane packing (Fig.1, 2). It is then collected at the end of the packing using a manifold and is guided outside of the catheter through an outlet pipe (Fig.1, 3). The assembly of the catheter has an overall length of 330 mm and a maximum outer diameter of 14 mm.

The miniaturized blood pump with an outer casing diameter of 8.5 mm is designed to provide a blood flow ranging from 0.7 to 1.2 L/min through the membrane packing. Pressure drops of up to 300 mmHg can be compensated to guarantee sufficient blood flow for gas exchange in the membrane module.

The membrane module has a length of 125 mm and an outer diameter of 14 mm. Approximately 234 fibers (Membran Oxyplus® 90/200 PMP, 3M) were incorporated into the module. CO_2 transfer in the membrane module was investigated in [14].

The housing parts and the pump rotor of the prototype were 3D printed by a high resolution DLP resin printer. The pump shaft is made of hardened steel with a diamond-like carbon (DLC) surface and rotates in a hydrodynamic bearing made of polyether ether ketone.

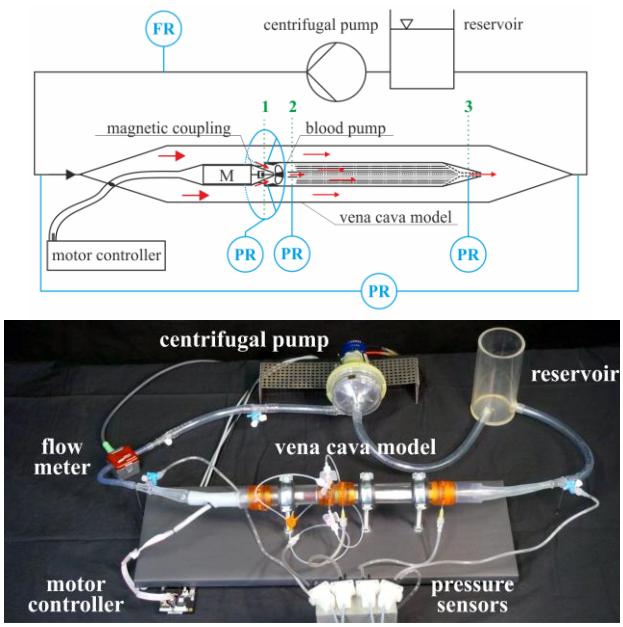

Figure 2: Top: schematic of the in-vitro recirculation loop. (1) pump inlet, (2) pump outlet, (3) membrane outlet pipe. Bottom: actual setup of the in-vitro recirculation loop with reservoir, centrifugal pump, clamp on flow meter (FR), vena cava model, inserted catheter and indwelling injection cannulas connected to pressure sensors (PR).

B. *In-vitro flow loop*

Performance tests of the blood pump integrated into the catheter housing were conducted in an in-vitro recirculation loop (Fig. 1). This loop consists of a reservoir, a centrifugal pump (BPX-80, Medtronic), a cylindrical-shaped acrylic tube

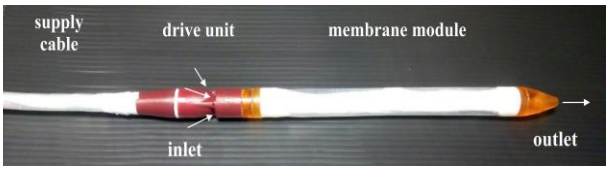

Figure 1: Catheter prototype with supply cable, drive unit and membrane module (from left to right).

that serves as a simplified model of the vena cava and a return hose for recirculation. The catheter prototype was co-axially placed inside the acrylic tube, which has an internal diameter of 25.5 mm. The assembly allows adjustment in the distance between catheter and tube by using flexible indwelling injection cannulas as pressure measuring channels.

As a substitute for blood a 60 vol.% water- and 40 vol.% glycerol-mixture was used, which had a density of 1090 kg/m^3 and kinematic viscosity 3.2 mm^2/s, which was determined according to ASTM D445 [15]. Water-glycerol solutions as Newtonian liquids have proven to be a suitable model for reproducing the Newtonian behavior of blood at strain rates above 100 s^{-1} [15], [16]. A clamp-on ultrasonic flow probe (SONOFLOW CO.55/080) monitored the flow rate (6 L/min) in the return hose. The pressure transducers (MPX5050 & MPX5500, NXP Semiconductors) were connected to the injection cannulas which were inserted perpendicular to the flow direction (Fig.1, PR). The static pressure was measured at each of the three pump inlet channels as well as pump and membrane outlets.

C. *Experiments*

The experiments were conducted in three steps. First, the characteristics of the pump were determined at different rotational speeds. This was done as a preparatory experiment (outside the vena cava model). The blood pump was supplied with water-glycerol by a feed-stream-adapter, connecting the feed hose to the pump inlets. A return hose was directly connected to the pump outlet. On the return hose a flow- rate sensor and a throttle, substituting the membrane packing, was clamped on. Pressure difference between pump in- and outlet was measured (Fig. 3).

In a second preparatory experiment, the throttle was exchanged by the membrane module, which was directly connected to the pump housing. The pressure differences over the pump and the membrane module were measured at pump speeds between 26000 to 38000 rpm in 1000 rpm steps. This set-up allows to determine a correlation between flow rate through the catheter and pressure loss over the catheter, as a function of the rotational speed of the catheter pump.

The flows outside the catheter and through the membrane were investigated in a third experiment by employing the complete in-vitro recirculation loop. Tests were conducted for different rotational speeds of the catheter pump (26000 – 38000 rpm in 1000 rpm steps) and three radial positions of the catheter (central position, 1.5 mm and 3.0 mm minimal distance to vena cava wall). Absolute pressure was measured at pump inlet, pump outlet and membrane outlet (Fig. 1). Differential pressure was measured at vena cava in- and outlet. The overall flow through the loop was measured directly with the flow probe.

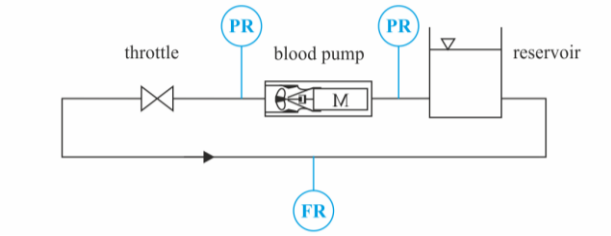

Figure 3: Schematic of the first experimental set-up for measuring the pump characteristics.

Based on the correlation determined in the second test setup, the flow through the membrane module was estimated using pressure measurement data. All experiments were conducted at constant room temperatures of about 298 K.

D. Computational Fluid Dynamics

OpenFOAM 4.1 (ESI Group, Paris, France) was used to solve the steady incompressible laminar Navier-Stokes equations. The water-glycerol-mixture was modeled as a single-phase Newtonian fluid using the measured mixture viscosity. Surrounding outer flow of catheter for three different minimal wall distances (central position, 1.5 mm and 3.0 mm) in the cylindrical test section was simulated. For initial studies, the flow inside the catheter was neglected. Inflow into the pump and outflow at the catheter end were therefore approximated with additional boundary conditions.

Pump inlet boundary was generated by the three inlet channel cross sections of the pump housing. Membrane outlet boundary was defined via the cross-sectional area of the outlet duct at the downstream end of the catheter. Both boundaries were fitted to the position of the pressure measuring channels (Fig. 1, 1 & 3).

On all outlet boundaries of the simulated domain (pump inlet and test section outlet) a uniform pressure value and a velocity gradient of zero was applied as boundary condition. At the pump inlet a static suction pressure was used to generate an outflow of the simulation domain of 1 L/min at central catheter position. This pressure was determined using an L-BFGS-B optimization algorithm [18]. At all inlets of the domain (membrane outlet and test section inlet), pressure was determined via a zero-gradient condition. Uniform inlet velocities were set to equal a fixed flow rate. Total test section inflow was set to 6 L/min. Inflow at the membrane outlet was iteratively matched to the outflow at pump inlet, the later calculated based on the suction pressure boundary condition described above.

III. Results

A. Experimental Results

In Fig. 4 the characteristic curves of the blood pump are shown for rotational speeds ranging between 26000 and 38000 rpm. Flow rates as a function of pump speed n vary from 0.8 to 1.0 L/min for pressure differences between pump out- and inlet from 130 to 300 mmHg.

The correlation between pressure drop (Δp) over the membrane module and flow (Q) through the membrane module was determined for flow rates ranging from 0.8 to 1.0 L/min.

$$\Delta p = 206.15 \cdot Q^{3.4346} \quad (1)$$

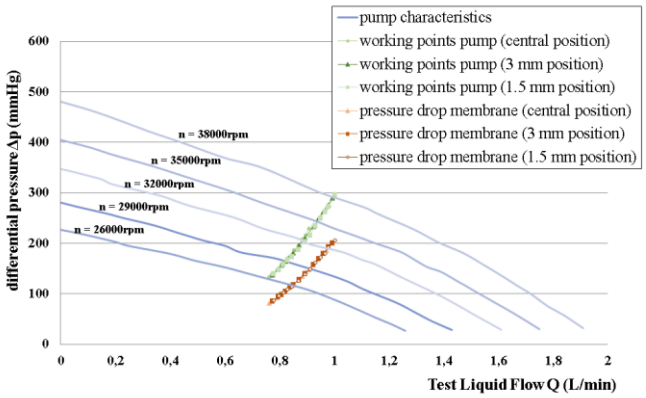

Figure 5: Pump characteristics (blue), pressure drop in membrane module (red) and pump working points (green) for various catheter positions and pump speeds n.

Measurement data of the in-vitro recirculation loop experiments are illustrated in Fig. 4. It shows the total pressure drop over the membrane as a function of the catheter in flow rate (red). The total pressure rise generated by the pump to deliver this catheter in flow is marked in green. Both curves were measured for various catheter positions and different blood pump rotational speeds. Catheter inflow rate was estimated using (1) and increases from 0.8 to 1.0 L/min depending on rotational pump speed (26000 to 38000 rpm). There is a significant difference between total pressure rise (green) and total pressure drop (red) ranging from 61 mmHg (25 mmHg static pressure) at 0.8 L/min to 98 mmHg (43 mmHg static pressure) at 1.0 L/min. This difference is equivalent to 41 % respectively 32 % of pump generated total pressure rise. As seen in Fig. 4 the results of the experiments show no detectable influence of catheter positioning on the catheter inflow.

B. Computational Fluid Dynamics Results

The basic and simplified simulations run stable and converge fast, usually within 15 min in a parallel run on four processor cores (AMD FX 8 core processor). They show laminar flow behavior. As can be seen in Fig. 5, peak velocities are reached in the outlet jet of the catheter (4.5 m/s) whereas the catheter bypass flow remains relatively slow with velocity magnitudes less than 0.4 m/s. Decay of the jet in the simulation domain is negligibly small. According to the simulation, reduction of wall distance between vena cava and catheter leads to the development of asymmetric flow patterns and a 15 % decrease of catheter in flow (see table 1).

Static pressure drop in the cylindrical part of the test section is lower than 1 mmHg. The main static pressure drop can be assigned to the cone outlet adapter at the end of the

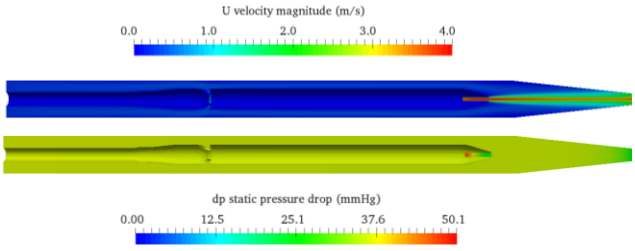

Figure 4 Contour plots of static pressure and velocity magnitude in the cylindrical test section and outlet cone.

cylindrical test section (35.5 mmHg). Significant pressure losses can also be seen in the outlet pipe of the catheter (11.5 mmHg). A static suction pressure of 4.6 mmHg is necessary to generate a catheter inflow of 1 L/min. CFD analysis also shows strain rates above 100 s^{-1} in the surrounding flow, whereas peak rates of 3000 s^{-1} are achieved at the thin boundary between exhaust jet and surrounding flow.

IV. Discussion

Experiments on the characteristics and performance of the catheter device for CO_2 reduction in blood were conducted in an in-vitro recirculation loop, which included a vena cava model as primary part of the test section. Main elements of the catheter prototype were manufactured using a DLP resin printer. Extensive experimental test runs showed that the catheter prototype is running in stable and reliable manner. The achieved flows of 0.8 -1.0 L/min are in the required flow range.

According to the measurement results, there is a significant pressure loss (32 – 41 % of pump generated total pressure difference) in the vena cava in addition to the pressure loss induced by the membrane module. CFD results indicate that these pressure losses may be caused by the conical shape of the vena cava's end part, whereas pressure losses over the length of the catheter are lower than 1 mmHg. Furthermore, velocities in the exhaust jet are exceeding velocities in the surrounding flow by a factor of ten, causing unfavorable mixing behavior and unnecessary pressure losses. These pressure losses can be diminished by either optimizing the outlet by designing a central diffusor or allowing for multiple outlets on the shell side of the membrane module.

Contrary to the CFD simulations, in the experiments, variations of the distance between catheter and vena cava wall led to no detectable reduction of catheter inflow rate. This indicates that either the pump must be resolved by the CFD simulation or a more advanced model for the pump inflow should be implemented. Parts of the feed supply hose and the connector to the cylindrical test section will also be added to the simulation at a later stage. For further simulations a turbulence model (e.g. k-ω SST turbulence model) could improve the accuracy of the model. Utilizing particle image velocimetry (PIV) in future tests will allow to further validate both, experimental and simulation data.

Regarding the experiments, flexible tubing materials, e.g. latex or silicone for the vena cava model, could add compliance as to better represent physiological conditions. More advanced 3D printing and manufacturing technologies as well as metal alloys and technical ceramics would allow to further reduce catheter and drive unit dimensions to completely comply with anatomical limitations. With strain rates above 100 s^{-1} in the examined flow, blood rheology has Newtonian behavior [16] and can be substituted by a water-glycerol mixture in the in-vitro recirculation loop [17]. Evaluation of blood hemolysis, due to higher mechanical stresses in pump, catheter outlet and membrane packing, is going to be a key aspect of future experiments. Modifications in the membrane module for optimal gas exchange may further influence the flow behavior.

TABLE I Comparison Experiments And CFD

Wall distance	*Flow rate experimental*[a]	*Flow rate CFD*
Central position	0.99 L/min	1.00 L/min
3.0 mm	0.99 L/min	0.97 L/min
1.5 mm	1.00 L/min	0.86 L/min

a. pump speed n = 38000 rpm.

In conclusion, the simulations provide valuable information on velocity and pressure fields, for a better understanding of the impact of the membrane catheter in the physiological blood flow in the vena cava. They qualify as a basis for fast and simple testing during catheter prototyping and allow future optimizations of the catheter including the catheter outlet. Together with the flexibility of additive manufacturing methods, a faster and more efficient prototyping process can be implemented.

V. References

[1] P. ROCK, "Respiratory Diseases," *Anesth. Uncommon Dis. Expert Consult-Online Print*, p. 137, 2012.

[2] T. Ferkol and D. Schraufnagel, "The Global Burden of Respiratory Disease," *Ann.Am. Thorac. Soc.*,vol. 11,no. 3, pp.404–406, Mar. 2014.

[3] D. Schnell *et al.*, "Noninvasive mechanical ventilation in acute respiratory failure: trends in use and outcomes," *Intensive Care Med.*, vol. 40, pp. 582–591, Feb. 2014.

[4] L. Pinhu, T. Whitehead, T. Evans, M. Griffiths, "Ventilator-associated lung injury," *The Lancet*, vol. 361, no. 9354, pp. 332–340, Jan. 2003.

[5] J. Villar *et al.*, "The ALIEN study: incidence and outcome of acute respiratory distress syndrome in the era of lung protective ventilation," *Intensive Care Med.*, vol. 37, no. 12, pp. 1932–1941, Dec. 2011.

[6] J.-M. Boles et al., "Weaning from mechanical ventilation," Eur. Respir. J., vol. 29, no. 5, pp. 1033–1056, May 2007

[7] G. Makdisi and I. Wang, "Extra Corporeal Membrane Oxygenation (ECMO) review of a lifesaving technology," *J. Thorac. Dis.*, vol. 7, no. 7, pp. E166–E176, Jul. 2015.

[8] W. Tao *et al.*, "Performance of an intravenous gas exchanger (IVOX) in a venovenous bypass circuit," *Ann. Thorac. Surg.*, vol. 57, no. 6, pp. 1484–1491, Jun. 1994.

[9] J. F. Golob *et al.*, "Acute In Vivo Testing of an Intravascular Respiratory Support Catheter," *ASAIO J.*, vol. 47, no. 5, pp. 432–437, Oct. 2001.

[10] R. G. Jeffries, B. J. Frankowski, G. W. Burgreen, and W. J. Federspiel, "Effect of Impeller Design and Spacing on Gas Exchange in a Percutaneous Respiratory Assist Catheter," *Artif. Organs*, vol. 38, no. 12, pp. 1007–1017, Dec. 2014.

[11] J. G. Riess, "Oxygen carriers ('blood substitutes')--raison d'etre, chemistry, and some physiology," *Chem. Rev.*, vol. 101, no. 9, pp. 2797–2920, Sep. 2001.

[12] D. R. Spahn, "Blood substitutes Artificial oxygen carriers: perfluorocarbon emulsions,"*Crit.Care*, vol.3,no.5,pp.R93–R97, 1999.

[13] C. Janeczek and M. Hinteregger, "Magnetic Coupling," Austrian patent application: A50343/2014.

[14] M. Harasek, B. Haddadi, C. Jordan, M. Gföhler, C. Janeczek, A. Karabegovic, L. Futter, C. Krenn, S. Neudl, R. Ullrich: "Intracorporeal Membrane Catheter for CO2 Reduction in a Blood-Membrane Contactor"; Int. J of Artificial Organs, 40 (2017), 8; p. 414.

[15] ASTM International, *ASTM D445-17a, Standard Test Method for Kinematic Viscosity of Transparent and Opaque Liquids (and Calculation of Dynamic Viscosity)*. West Conshohocken, PA, 2017.

[16] E. W. Merrill, "Rheology of blood," *Physiol. Rev.*, vol. 49, no. 4, pp. 863–888, Oct. 1969.

[17] M. Y. Yousif, D. W. Holdsworth, and T. L. Poepping, "A blood-mimicking fluid for particle image velocimetry with silicone vascular models," *Exp. Fluids*, vol. 50, no. 3, pp. 769–774, 2011.

[18] B. Lukitsch, *Programming of a Framework for the Parameter Optimization of CFD Simulations and the k-epsilon Turbulence Model as an Example*. Vienna: Masterthesis, TU Wien, 2017.